

## Research Article

# Porous Bioactive Glass Scaffolds for Local Drug Delivery in Osteomyelitis: Development and *In Vitro* Characterization

Chidambaram Soundrapandian,<sup>1,2</sup> Someswar Datta,<sup>1</sup> Biswanath Kundu,<sup>1</sup> Debabrata Basu,<sup>1</sup> and Biswanath Sa<sup>2,3</sup>

Received 7 May 2010; accepted 12 November 2010; published online 24 November 2010

**Abstract.** A new bioactive glass-based scaffold was developed for local delivery of drugs in case of osteomyelitis. Bioactive glass having a new composition was prepared and converted into porous scaffold. The bioactivity of the resulting scaffold was examined by *in vitro* acellular method. The scaffolds were loaded with two different drugs, an antibacterial or antifungal drug. The effects of the size of the scaffold, drug concentration, and dissolution medium on drug release were studied. The scaffolds were further coated with a degradable natural polymer, chitosan, to further control the drug release. Both the glass and scaffold were bioactive. The scaffolds released both the drugs for 6 weeks, *in vitro*. The results indicated that the bigger the size and the higher the drug concentration, the better was the release profile. The scaffolds appeared to be suitable for local delivery of the drugs in cases of osteomyelitis.

**KEY WORDS:** bioceramics; bone infection; drug release; organic–inorganic composite; skeletal drug delivery.

## INTRODUCTION

Osteomyelitis, an inflammatory process accompanied by bone destruction, is caused by infective microorganisms (1). Conventional drug delivery systems often fail to maintain therapeutically effective drug concentrations at the site of infection, as the area is moderately perfused and almost devoid of blood supply. On the other hand, local drug delivery systems, which could release drugs in a prolonged and controlled fashion, may establish higher drug concentrations at the intended site with no or minimal drug concentration in the systemic circulation (1–3).

Local drug delivery systems in the treatment of osteomyelitis are expected to release the drug for at least a period of 4–6 weeks (1,4). Although various polymers are able to prolong drug release, they present formidable limitations such as follow-up surgery in case of nonbiodegradable polymers, high cost, tissue reactions, and/or immunological considerations depending upon the source of origin (2). In addition, hazardous organic solvents are often required in the formulation of delivery devices based on polymers. These factors triggered the search for other suitable carrier materials.

Bioceramic carriers are fast becoming a replacement for polymers in drug delivery, especially when local delivery of drugs in the bone is intended. Bioceramic entities such as

tricalcium phosphate, hydroxyapatite, and bioactive glass have been used for tissue engineering and drug delivery (1,5). Bioactive glasses are a class of bioceramics that comprise of a group of surface reactive glass/glass-ceramic which are bioactive, osteoconductive, and osteoinductive (6,7). Unlike hydroxyapatite implants, bioactive glass implants have not been studied extensively for drug release. Recently, porous (macroporous) bioactive glass scaffolds were developed as local drug delivery system in our laboratory. However, *in vitro* release studies revealed the inability of the scaffolds to provide release for 4 weeks in a regulated manner.

This work envisaged the development of a new bioactive scaffold which could deliver drugs locally into the bone for extended period of time. The scaffold was examined for *in vitro* acellular bioactivity and loaded with gatifloxacin and fluconazole. The effect of various formulation factors like size of the scaffold and concentration of the drug on drug release in phosphate-buffered saline (PBS) and simulated body fluid (SBF) were investigated. The effect of coating the scaffold with a degradable natural polymer, chitosan, on drug release was also studied. Gatifloxacin HCl, an antibacterial drug suitable for bacterial osteomyelitis, and fluconazole, an antifungal drug preferred for fungal osteomyelitis, were selected as model drugs.

## MATERIALS AND METHODS

Quartz (MERCK, Darmstadt, Germany), sodium carbonate (MERCK, Mumbai, India), calcium carbonate (MERCK, Mumbai, India), diammonium hydrogen orthophosphate (MERCK, Darmstadt, Germany), and chitosan (ALDRICH, Milwaukee, WI, USA) were used as received.

<sup>1</sup> Bioceramic and Coating Division, Central Glass & Ceramic Research Institute, Raja S C Mallick Road, Kolkata, 700032, India.

<sup>2</sup> Department of Pharmaceutical Technology, Jadavpur University, Kolkata, 700032, India.

<sup>3</sup> To whom correspondence should be addressed. (e-mail: biswanath-sa2003@yahoo.com)

All the chemicals used were of AR grade or equivalent. Drugs were received as gift samples from Cross Medineeds Pvt. Ltd., India.

### Preparation of Bioactive Glass

Bioactive glass (SSS) was prepared by conventional glass melting procedure in a platinum crucible in ambient atmosphere at 1,350°C with an oxide composition of 45% (w/w) SiO<sub>2</sub>, 21.2% (w/w) CaO, 26% (w/w) Na<sub>2</sub>O, and 7.8% (w/w) P<sub>2</sub>O<sub>5</sub>. After homogenization of glass melt, the molten mass was quenched in distilled water, to yield glassy flakes, which were finally dried and stored.

### Characterization of Bioactive Glass

Fourier transform infrared (FTIR) spectrum of the bioactive glass was recorded in a FTIR spectrophotometer (Spectrum 100, PerkinElmer, Waltham, MA, USA). Powdered glass was mixed with KBr and converted into disk at 10-ton pressure using a hydraulic press. The spectrum was recorded at ambient temperature within 4,000–400 cm<sup>-1</sup> wave numbers at a resolution of 2 cm<sup>-1</sup>.

X-ray diffraction (XRD) analysis was performed with an X-ray diffractometer (X'Pert Pro, Phillips Analytical, The Netherlands). Powdered glass was scanned from 10° to 80° diffraction angle (2θ) range under the following conditions: source, monochromatic Cu Kα1 radiation (λ = 1.5406 Å); voltage, 40 kV; current, 35 mA, scan speed, 2° m<sup>-1</sup>.

Acellular *in vitro* bioactivity of the SSS powders was evaluated in SBF having an ionic composition similar to that of human plasma (2). SBF fluid containing SSS powder in a concentration of 1.5 mg/mL was placed in well-closed polystyrene bottles maintained at 37°C. Samples were collected after 1, 3, and 7 days and analyzed by FTIR.

### Preparation of Porous Bioactive Glass Scaffolds

SSS glass powder was mixed with equal quantity of porogen (naphthalene) and pressed into cylindrical blocks by cold-isostatic press (EPSI, Temse, Belgium) at 150 MPa for 1 min. Subsequently, blocks were turned and cut into circular disks of varying dimensions with a lathe and a low speed saw (Isomet, BUEHLER, Lake Bluff, IL, USA). Thereafter, the shaped samples were subjected to graded temperatures (25–80°C) and finally fired at about 725°C for 3 min on a Pt-Rh plate and stored in a vacuum desiccator until further use.

### Characterization of Porous Scaffolds

Porosity of the blocks was measured by water displacement method (Archimede's principle), and pore size distribution was measured using a mercury porosimeter (PM60, Quantachrome, Boynton Beach, FL, USA) with applied pressure ranging between 0 and 3,000 psi, a contact angle of 140°, and a surface tension of 480 dyn/cm. Acellular *in vitro* bioactivity of SSS porous scaffolds was evaluated in the same way as that of bioactive glass. After definite time intervals,

the scaffolds were observed under scanning electron microscope (SEM; Stereoscan430i, Leo, UK). XRD analysis of the porous scaffolds was performed in a similar way as mentioned earlier in this article for bioactive glass.

Weight changes of the scaffold between two sampling points and the change in pH of the SBF during acellular *in vitro* bioactivity study were measured respectively with an analytical balance of accuracy ±0.1 mg (Sartorius AG, Goettingen, Germany) and a pH meter with platinum pH electrode (Sension1, Hach, Loveland, CO, USA). During the sampling point, scaffolds were taken out of the buffer, pat-dried with tissue paper, and dried in a hot air oven until it reached a constant weight. The samples were then stored in a tightly closed desiccator at room temperature, before initiation of next part of the study.

### Preparation of Drug-Loaded Porous Bioactive Glass Scaffolds

Scaffolds were loaded with gatifloxacin by vacuum infiltration method. A scaffold of known weight was immersed in drug solution, and a vacuum of 9.67 ton/in.<sup>2</sup> was applied for 20 min. After the stated period, vacuum was released and the scaffold was allowed to dry under ambient conditions.

The following variables were used to prepare drug-loaded scaffolds:

1. Size of the scaffold: Keeping the concentration of drug solution fixed at 25 mg/mL, the height of the scaffolds was varied from 3 to 12 mm.
2. Concentration of the drug solution: Keeping the height of the scaffold fixed at 12 mm, the concentration of the drug solution was varied from 6.25 to 25 mg/mL.
3. Type of drug: Scaffolds of 12 mm height were loaded with gatifloxacin or fluconazole by vacuum infiltration method with drug solutions of concentration 25 mg/mL.

Table I presents the code assigned to the scaffolds and the variables involved.

### Preparation of Chitosan-Coated Scaffolds

The drug-loaded scaffolds having a height of 12 mm were coated with 0.5% or 1.0% (w/v) chitosan solution.

### Determination of Drug Loading in Scaffolds

The amount of drug loaded in the scaffold was measured by determining the concentration of drug solution before and after the infiltration process (8). The concentration of drug solution was determined by suitably diluting an aliquot with the respective medium and analyzing in an UV spectrophotometer (PerkinElmer, Waltham, MA, USA) at 287 and 261 nm for gatifloxacin and fluconazole, respectively. The drug concentration was determined from the respective calibration curves constructed using known concentration of gatifloxacin and fluconazole.

Table I. Composition of Scaffolds

Scaffold code	Height of the scaffold (mm)	Concentration of the drug in loading solution (mg/mL)	Drug	Concentration of chitosan in coating solution (% , w/v)	Dissolution medium
SSS-1	3	25	Gatifloxacin	–	PBS
SSS-2	6	25	Gatifloxacin	–	PBS
SSS-3	12	25	Gatifloxacin	–	PBS
SSS-4	12	12.5	Gatifloxacin	–	PBS
SSS-5	12	6.25	Gatifloxacin	–	PBS
SSS-6	12	25	Fluconazole	–	PBS
SSS-7	12	25	Gatifloxacin	0.5	PBS
SSS-8	12	25	Gatifloxacin	1.0	PBS
SSS-9	12	25	Gatifloxacin	–	SBF

PBS phosphate-buffered saline, SBF simulated body fluid

Drug loading in scaffolds was determined from the following relationship

$$\text{Drug loading(\%)} = \left[ \frac{\text{Amount of drug in solution before loading} - \text{Amount of drug in solution after loading}}{\text{Weight of the scaffold, g}} \right] \times 100$$

### In Vitro Drug Release Studies

Drug-loaded scaffolds were immersed in 5 mL of PBS (pH 7.4) maintained at 37°C. Aliquots were removed at selected intervals from 24 h to 43 days and analyzed by UV spectrophotometry. Study was terminated when samples failed to release drug above 1.2 µg/mL/day or 43 days, whichever was earlier. The set limit value was averaged per day by dividing the measured concentration with the number of days between the sampling. *In vitro* drug release studies were conducted in a similar way in SBF (pH 7.4).

### Drug Release Kinetics

To study the drug release kinetics from SSS scaffolds, the *in vitro* drug release data of gatifloxacin in different dissolution mediums were fitted in various kinetic models: zero order (Eq. 2), first order (Eq. 3), Higuchi's model (Eq. 4), Hixon-Crowell model (Eq. 5), and Peppas-Korsmeyer (Eq. 6) models.

$$A = k_0 t \quad (2)$$

where  $k_0$  is the zero-order rate constant and  $A$  is the amount of drug released at time  $t$ .

$$\log AR = k_1 t / 2.303 \quad (3)$$

where  $k_1$  is the first-order rate constant and  $AR$  is the amount of unreleased drug at time  $t$ .

$$A = kt^{0.5} \quad (4)$$

where  $k$  is the Higuchi's constant reflecting the design variables of the delivery system.

$$(AR)^{1/3} = k_2 t \quad (5)$$

where  $k_2$  is the Hixon-Crowell constant

$$At/A_\infty = k_3 t^n \quad (6)$$

where  $k_3$  is the Peppas-Korsmeyer constant,  $At/A_\infty$  is the fractional solute release at time  $t$ , and  $n$  is the exponent indicative of the release mechanism (9). An exponent value of 0.45 or less and 0.89 or above indicate respectively Fickian diffusion and case II transport (typical zero-order release). Values between 0.45 and 0.89 indicate non-Fickian or anomalous (by both diffusion and erosion) release. All release tests were carried out in triplicate, and the results were expressed as mean  $\pm$  SD.

## RESULTS AND DISCUSSIONS

Quaternary glass systems containing SiO<sub>2</sub>, Na<sub>2</sub>O, CaO, and P<sub>2</sub>O<sub>5</sub> in certain compositions are known to be bioactive. Chemical compositions having SiO<sub>2</sub> <60 mol%, high Na<sub>2</sub>O and CaO contents, and a high CaO/P<sub>2</sub>O<sub>5</sub> ratio are expected to exhibit high bioactivity (10,11). In the present work, a new composition of bioactive glass has been developed to study its applicability for local drug delivery in bone. This new composition contains a relatively high amount of P<sub>2</sub>O<sub>5</sub>. Firstly, this would increase dissolution of glass, which in turn may extend drug release rate. Secondly, this will increase local concentration of PO<sub>4</sub><sup>3-</sup> ions, which may enhance subsequent growth rate of carbonated hydroxyapatite deposition to influence new bone matrix generation.

### Characterization of SSS Powder

The FTIR spectrum (Fig. 1) showed well-defined peaks of the stretching and bending vibrations of Si–O–Si bonds at around 468, 802, and 1,040 cm<sup>-1</sup>. In addition, the spectrum showed two peaks at 1,414 and 1,454 cm<sup>-1</sup>, which are the characteristic peaks of C–O group. The emergence of these two peaks could be due to the absorption of CO<sub>2</sub> from atmosphere even after thermal treatment. A similar observation has been reported with calcium phosphate silicate/wollastonite (12), and hence, storage in dessicator is advised. XRD patterns (Fig. 2) indicated the amorphous nature of SSS, which is desirable for *in vivo* applications (13).

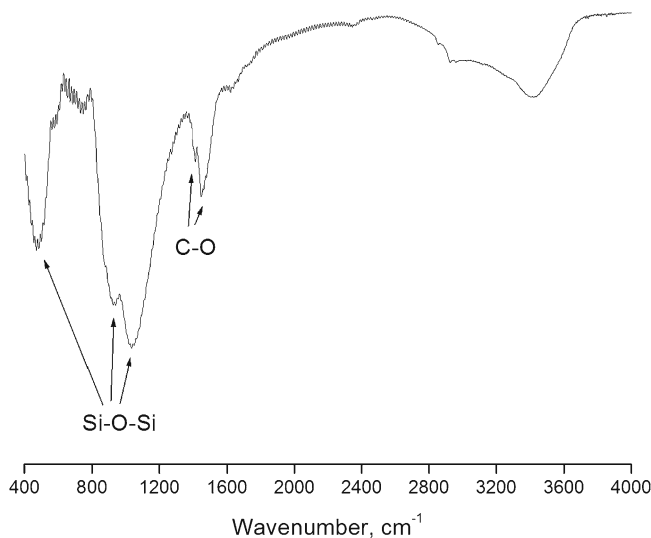


**Fig. 1.** FTIR spectrum of SSS powder

The *in vitro* acellular bioactivity of SSS glass was studied for a period of 1 week. Figure 3 illustrates the FTIR spectra of SSS glass before and after soaking in SBF for different periods (1, 3, and 7 days). Before soaking in SBF, the sample exhibited bending and stretching vibrations of Si-O-Si bonds at 468, 802, and 1,040 cm<sup>-1</sup>. After soaking in SBF for 1 day, a P-O vibrational bond at 566 cm<sup>-1</sup> was observed indicating the growth of amorphous phosphate. After 3 days, the said peak split into dual peaks at 566 and 603 cm<sup>-1</sup>, respectively, indicating the formation of crystalline phosphate. In addition, well-resolved peaks at 872, 1,418, and 1,487 cm<sup>-1</sup> assigned to C-O vibrational bands and 962 and 1,040 cm<sup>-1</sup> assigned to the crystalline P-O bonds could be observed indicating the formation of hydroxycarbonate apatite (HCAp). The mechanism of bonding of bioactive glasses with living tissues has been reported to be associated with the development of a layer consisting of carbonate-containing hydroxylapatite on the surface of the materials (14).

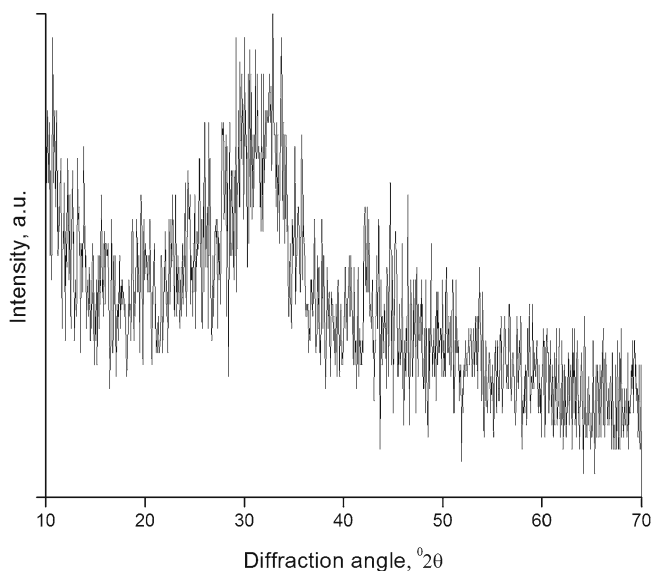


**Fig. 2.** XRD spectrum of SSS powder

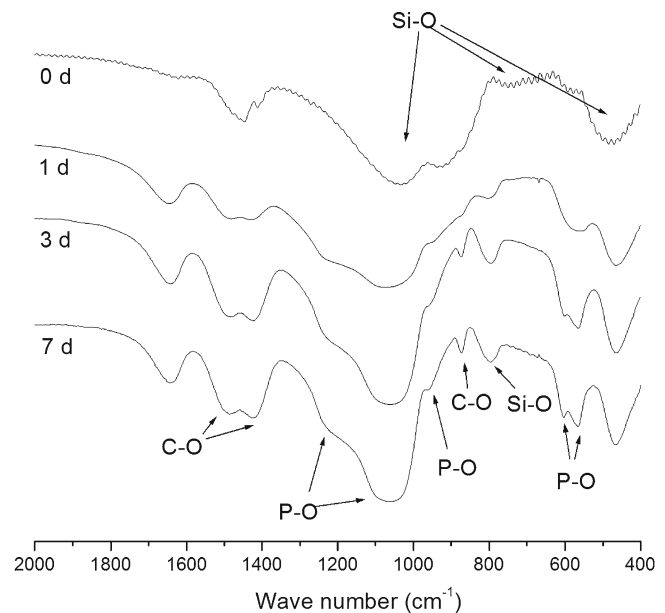


**Fig. 3.** FTIR spectra of SSS glass subjected to acellular *in vitro* bioactivity study at various periods

### Characterization of Porous Scaffolds

Porous SSS scaffolds were prepared by selecting naphthalene powder (as a porogen) of a particular size range (less than 296 μm). The bulk density of the SSS scaffolds was 0.844 (±0.09) g/cc. The true porosity and closed porosity were calculated to be 68.72% (±3.13%) and 4.15% (±1.01%), respectively, with an apparent porosity of 63.67% (±2.21%). These values are in the range generally agreed for rapid osteointegration (15). However, porosity and porous nature of the scaffolds can be manipulated by the properties of porogen and the sintering temperature of the scaffold (1,5). Selecting naphthalene of a particular size range and sticking to a fixed sintering procedure shall help to control these properties between batches.

Figure 4 presents the pores size distribution chart of porous SSS scaffolds. The pores were unimodal and predominantly in the range of 10–70 μm, indicating that they were suitable for drug delivery applications (1), as small pores are known to facilitate high adsorption of drug and to sustain the release better than the larger pores (16).

Figure 5 reveals the SEM images of SSS scaffolds subjected to *in vitro* bioactivity studies at various time points. The structure was intact for the entire study period. However, the surface exhibited significant changes before (0 days, SEM magnification ×5,000) and after soaking (1 day, SEM magnification ×20,000; 3 and 7 days, SEM magnification ×25,000) in SBF for different time. After soaking in SBF for 1 day, the entire surface was covered with apatites. After 3 days, the surface appeared to be covered with a mat and smaller clusters joined to form cauliflower like growth. At the end of 7 days, the deposits appeared as plates stacked upon and with spikes of growing crystals. Pores in micrometer range were also visible that were created either during fabrication or during deposition of apatites.

Figure 6 represents XRD spectra of surface deposits on SSS scaffolds, following *in vitro* bioactivity studies. Initially,

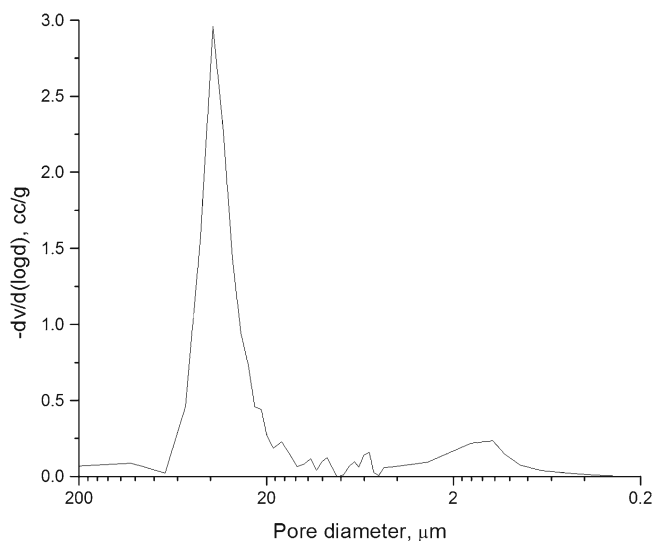


Fig. 4. Pore size distribution in SSS scaffolds

the scaffolds appeared to be amorphous. After incubation in SBF, new strong peaks at  $26^\circ$  and  $32^\circ$  of  $2\theta$  corresponding to good crystallinity of HCAp (JCPDS 04-0697) appeared, and the intensity of the peaks increased with time. This result confirmed that the scaffold was amorphous initially and the surface converted into crystalline state due to deposition of HCAp.

Figure 7 depicts the changes in pH and weight gain of SSS scaffold on exposure to SBF. A total gain of about 5.14% ( $w/w$ ) was observed at the end of the 4-week study period.

Unlike polymers, bioactive entities favor apatite deposition, and hence, over a period, weight gain of these scaffolds is obvious. It could be observed from the figure that the weight gain in the initial first week was very low, possibly due to a faster leaching of ions such as  $\text{Si}^+$ ,  $\text{Ca}^{2+}$ ,  $\text{Na}^+$ , and  $\text{PO}_4^{3-}$  from the scaffold than the deposition of apatites. From the second week to the fourth week, it was almost linear. Similar results of weight gain have been reported for bioactive tricalcium phosphate (17) and bioglass-polymer composite (18). The figure also shows a steep increase in the pH of the SBF solution from 7.4 to 8.76 in the first week. The high value was comparable with the result of other workers (19). However, for the rest of the study period, the pH was found to gradually decrease to a final value of 8.47. The increase in pH was due to the leaching of ions as  $\text{Ca}^{2+}$  and  $\text{Na}^+$  from the scaffold and is advantageous, as it is known to create a favorable atmosphere for apatite deposition.

#### Loading and *In Vitro* Drug Release Studies

The drug loading efficiency was calculated to be 2.5%. For *in vitro* drug release, cutoff limit of drug was fixed at ten times the minimum inhibitory concentration (MIC) of *Staphylococcus aureus*. The acceptable MIC ranges for *S. aureus* (ATCC 29213) is 0.03 to 0.12  $\mu\text{g}/\text{mL}$  for gatifloxacin (20). Hence, the cutoff limit was fixed at 1.2  $\mu\text{g}/\text{mL}/\text{day}$ . The intention was to deliver drug not only above MIC but also above biofilm eradication concentration. Biofilms are the main cause for relapse of infection, and generally more than ten folds the MIC to kill planktonic cells is required (1).

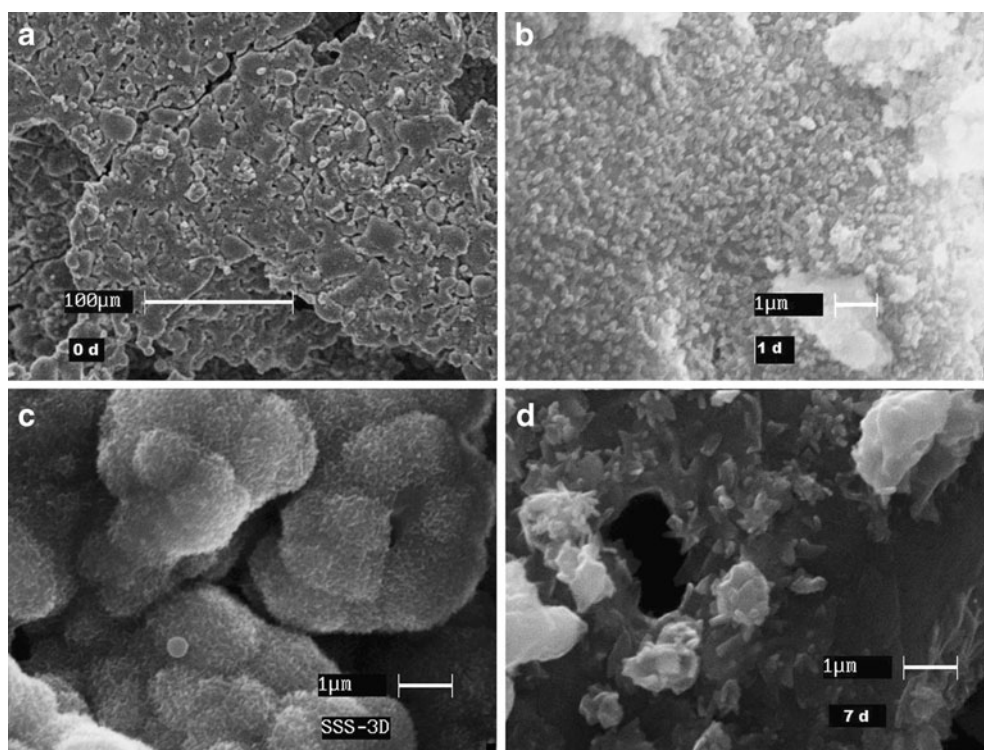
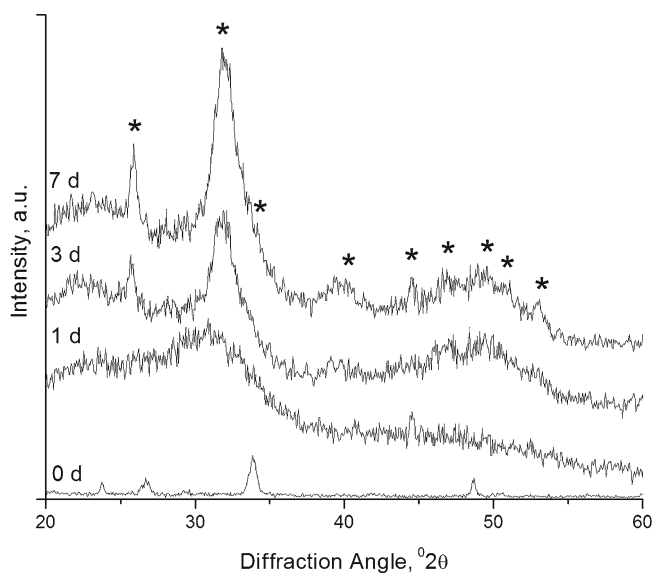


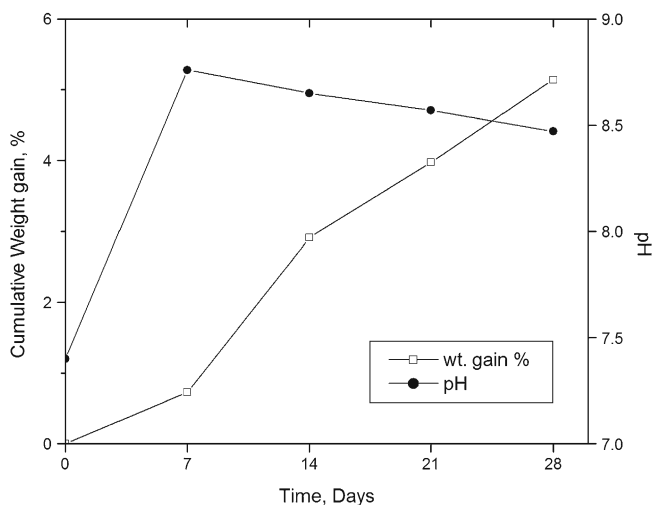
Fig. 5. SEM images of SSS scaffold surface subjected to acellular *in vitro* bioactivity study at various periods (0 d day 0, 1 d after 1 day, 3D after 3 days; 7 d after 7 days; SEM magnification: a 0 day ( $\times 5,000$ ), b 1 day ( $\times 20,000$ ), c 3 days ( $\times 25,000$ ), d 7 days ( $\times 25,000$ ))



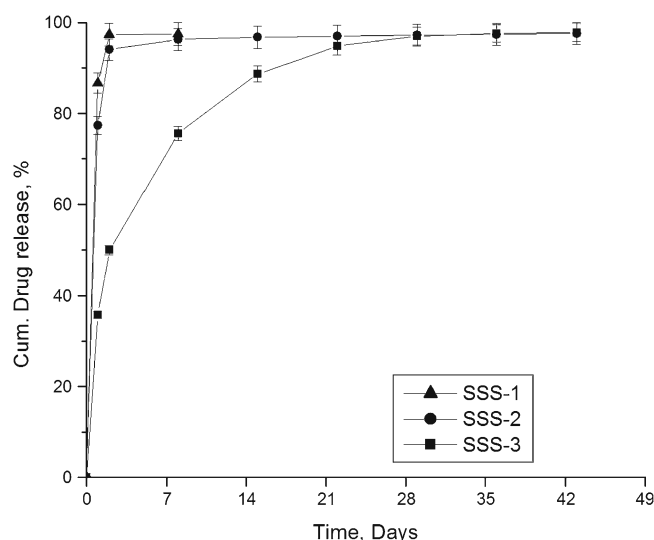
**Fig. 6.** XRD spectra of SSS scaffold surface deposit obtained at various periods of acellular *in vitro* bioactivity study (asterisk indicates characteristic peaks of HCAp)

Figure 8 presents the release profiles of gatifloxacin from various sized scaffolds. Among the three scaffolds, SSS-1 released the entire drug in 8 days. The formulations SSS-2 and SSS-3 were found to release the drug for the entire study period and above the set limit ( $1.2 \mu\text{g}/\text{mL}/\text{day}$ ). However, SSS-2 released more than 75% of the drug in the first day and about 94% in 2 days. On the other hand, although SSS-3 released a considerable amount of drug in the first day, it sustained the release better than the other two formulations. As the scaffold height increases, the path length to exit out for the drug molecule also increases. This eventually could lead to a much extended release profile. Hence, SSS-3 scaffold was selected for further investigations.

Figure 9 presents the release profiles of gatifloxacin from scaffolds prepared by immersing in drug solutions of varying concentrations. Of the studied three formulations, SSS-5 which was prepared by immersing in drug solution having



**Fig. 7.** Pattern of change in the weight of SSS scaffolds and the change in pH of the SBF employed in acellular *in vitro* bioactivity over the period of study



**Fig. 8.** Effect of scaffold size on drug release

the lowest concentration released 99% in just 2 days. Formulation SSS-4 could not sustain the release for entire study period and released more than 90% of drug in 8 days. However, formulation SSS-3 was found better in sustaining the drug release for extended period. Decrease in the concentration of drug in the loading solution resulted in lower entrapment of drug in the SSS scaffold (data not presented here). When a scaffold is immersed in a dilute drug solution, lesser number of drug molecules will enter into the pores, and hence, the pore channels of the scaffolds would contain fewer amounts of drug molecules. As a result, the drug molecules will experience less resistance for diffusion resulting in faster drug release.

Figure 10 compares the release profiles of gatifloxacin (SSS-3) and fluconazole (SSS-6) from SSS scaffolds. Both the drugs were found to be released over the entire study period of 43 days. Though the release of fluconazole was higher in the initial periods, the release slowed down and was found to be less than that of gatifloxacin after 7 days. While 91%

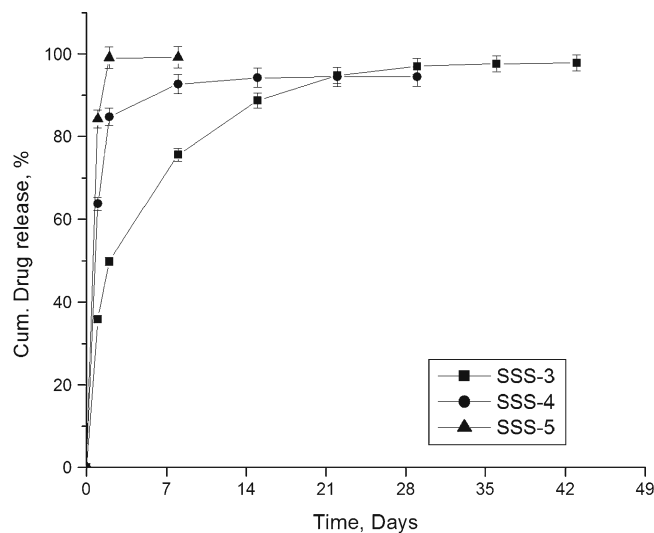


**Fig. 9.** Effect of concentration of drug in loading solution on drug release

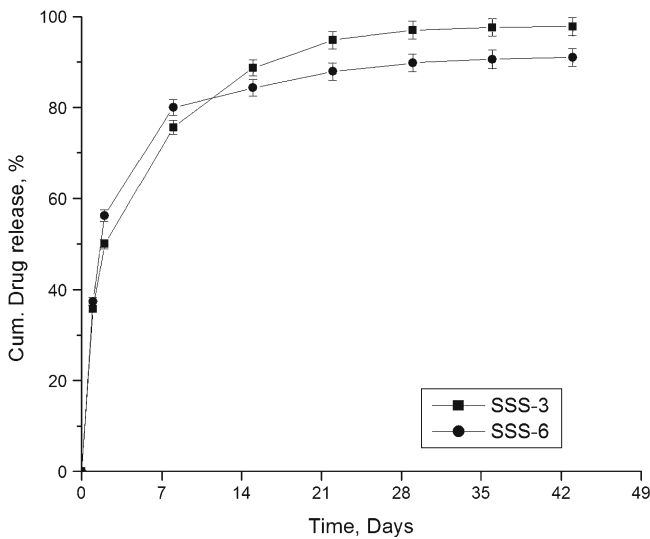


Fig. 10. Release profiles of two different drugs

fluconazole was released at the end of study period, 98% gatifloxacin was found to be released during the same period. The release of fluconazole was found to be better sustained than gatifloxacin possibly due to stronger hydrogen bonding of fluconazole.

Bioceramic scaffolds act more like a reservoir and drug molecules exist in the scaffolds in four different states (21). A considerable part of drug molecules is attached to the exterior surface of the bioactive glass scaffold while the major part is trapped in the pore channels where drug molecules exist in three different states. One part of the drug molecules exists at the pore channel openings, while the rest exist in the pore channels with or without bonding to the pore wall surface. Gatifloxacin or fluconazole were loaded in SSS scaffolds by immersing the scaffolds in drug solution and applying negative pressure. This results in the attachment of drug molecules in the pore channels and on the surface. In addition, both the drug molecules contain highly electronegative atoms/groups like F, N, and OH, which could form

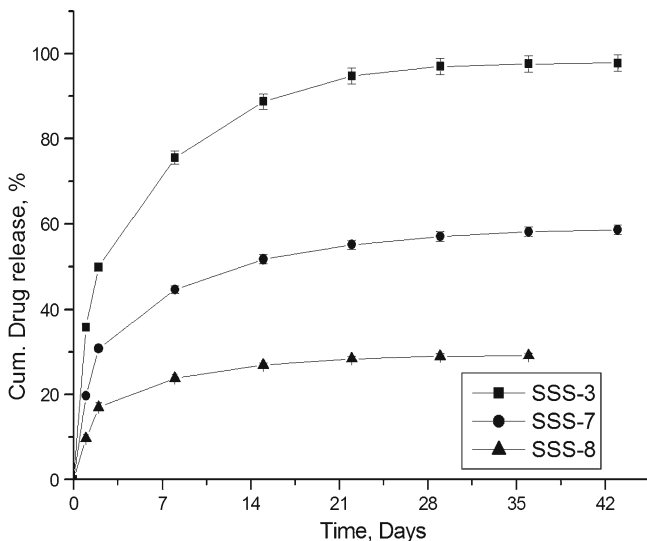


Fig. 11. Effect of coating and concentration of polymer solution on drug release

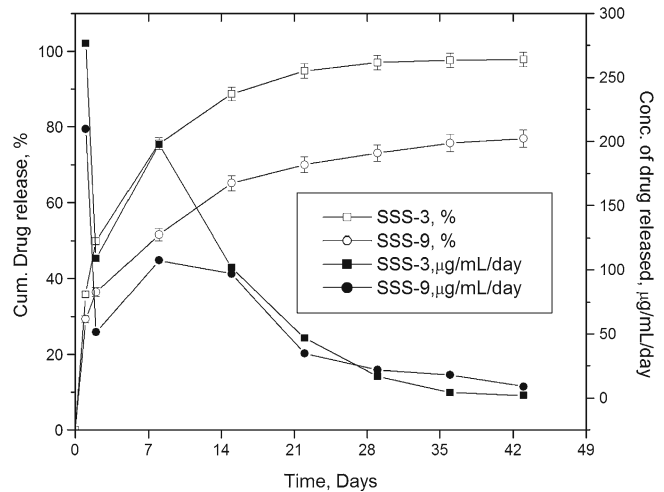


Fig. 12. Effect of dissolution medium on drug release

hydrogen bonds with Si-OH and P-OH groups in the scaffold or pore wall surface. Hence, it is obvious that the drug molecules adhered on the surface would be released faster, while those inside the pore channels would be released in a sustained fashion, as the drug has to diffuse through the channel.

Though SSS scaffolds were capable of releasing gatifloxacin and fluconazole for more than 6 weeks above the set limit, a considerable part of the drugs was released in 1 day. Coating the scaffolds could significantly reduce this burst release, and coating bioceramic scaffolds with polymer also results in the formation of organic-inorganic composite scaffolds. Chitosan was selected, as it is a natural polymer with excellent biocompatibility, nontoxicity, biodegradability, and bioresorbability (22–24). These properties along with their various biological activities as antibacterial, antifungal, haemostatic, and wound healing (25–27) make it an interesting polymer for selection. The effect of coating of SSS scaffolds with chitosan on drug release was compared with SSS-3. Figure 11 illustrates the release of gatifloxacin from uncoated (SSS-3) and coated (SSS-7 and SSS-8) scaffolds. Though coating of the scaffolds were able to reduce the burst release of drug significantly and provide extended release during the study period, SSS-8 formulation which was coated with highest concentration of chitosan (1%, w/v) failed to maintain the set limit (1.2 µg/mL/day) in the last week. On the other hand, SSS-7, coated with 0.5% chitosan, was able both to reduce the initial day release and to maintain the drug release concentration above the set limit for the entire study period. Though coating could be applied successfully to control drug release, the presence of polymer coat on bioceramics may affect bioactivity, by delaying the process (2).

Drug release studies are generally conducted in PBS as dissolution medium (1,2). However, bioceramics may react with SBF and form apatites on the surface, which could alter drug release. The effect of dissolution media on drug release was studied using SSS-3, and the results are shown in Fig. 12. The difference in release profiles started from the first 24 h, itself. Drug release in SBF was lower than that in PBS, and the difference became more prominent with progress in time. While SSS-3 released about 35% of drug in the first 24 h, SSS-

**Table II.** Modeled *In Vitro* Release Kinetics

Formulations	Zero-order $R^2$	First-order $R^2$	Higuchi $R^2$	Hixon–Crowell $R^2$	Peppas–Korsmeyer	
					$R^2$	$n$
SSS-3	0.7275	0.9428	0.8818	0.7275	0.9572	0.35
SSS-9	0.8375	0.9158	0.9529	0.8703	0.991	0.27

9 released only about 29%, both lower than the release (78%) reported earlier for the same drug from nonporous monolithic polymer-controlled systems (28). The maximum concentration of drug released per day from SSS-3 and SSS-9 were 276.5 and 209.6  $\mu\text{g/mL}$ , respectively, and the minimum concentration maintained to be 2.1 and 9.0  $\mu\text{g/mL}$  in PBS and SBF. At the end of study period, the amount of drug released in SBF was about 21% less than that in PBS, although the release of the drug was above the set concentration limit. This indicates that the same scaffold could deliver drugs successfully for a few weeks more in SBF. It is evident from the release profiles that the sustained release of drug from the scaffolds in SBF was also influenced by the formation of apatites. Though the formulation provided extended release profile above the set minimum limit, the release at maximum concentration is also a point of concern. High levels of many antibiotics have been reported to produce adverse effects on osteoblast function and bone regeneration. Tobramycin at concentrations of 400  $\mu\text{g/mL}$  decreased proliferation and at 10,000  $\mu\text{g/mL}$  caused death of osteoblasts (1). Though burst release from SSS-3 formulation was comparably many times lower, the effect of concentration on osteoblasts changes with drug (1). Hence, it would be better to ascertain the safety of high concentrations of the drug released before proceeding further to *in vivo* trials.

The theoretical analysis and models of drug release employed to describe release from polymers can also be applied for bioceramics (29). Comparing the results of various models studied (Table II), it was observed that the *in vitro* release of drug from SSS scaffolds followed a first-order release pattern irrespective of the media selected for this study. In addition, the mechanism of drug release from the SSS scaffolds was found to be diffusion-based following Higuchi's model. The erosion of the delivery system irrespective of dissolution medium had comparatively lesser effect on drug release as exhibited by Hixon–Crowell model. Better correlation with Higuchi's model was observed with SBF than PBS. Although erosion of SSS scaffolds happen in both the dissolution media, rebuilding of the scaffold took place in SBF. This was substantiated by the results of *in vitro* bioactivity and weight gain. This phenomenon probably maintained the effects of porosity and tortuosity on the diffusion of drug molecules. Finally, the result of Peppas–Korsmeyer model reconfirms the release mechanism of drug molecules to be diffusion controlled as the values of  $n$  varied from 0.27 to 0.35.

## CONCLUSION

Porous silica-based bioactive quaternary glass (SSS) scaffolds having a new composition were prepared for local

delivery of gatifloxacin and fluconazole in bone. *In vitro* acellular activity and instrumental characterization using FTIR and XRD confirmed the silica-based quaternary glass and the porous scaffolds to be bioactive. SSS scaffolds with unimodal pore distribution released the drugs for 6 weeks following first-order release with diffusion-based mechanism. The release was influenced by the size of the scaffold, concentration of drug solution, polymer coat, and dissolution medium. Among the formulations studied, SSS-3 was able to successfully extend the release of the drugs above the desired limit. These results indicate that the newly developed bioactive glass-based scaffolds could be a potential drug delivery system in osteomyelitis.

## ACKNOWLEDGMENTS

The authors wish to express their sincere thanks to The Director, CG&CRI, India for the kind permission and support for the successful completion of the research work. All the departments and technical staffs involved in characterization are duly acknowledged.

## REFERENCES

- Soundrapandian C, Datta S, Sa B. Drug-eluting implants for osteomyelitis. *Crit Rev Ther Drug Carrier Syst.* 2007;24:493–545.
- Soundrapandian C, Sa B, Datta S. Organic–inorganic composites for bone drug delivery. *AAPS PharmSciTech.* 2009;10:1158–71.
- Nandi SK, Mukherjee P, Roy S, Kundu B, De DK, Basu D. Local antibiotic delivery systems for the treatment of osteomyelitis—a review. *Mat Sci Eng C.* 2009;29:2478–85.
- Ouedraogo M, Semde R, Some IT, Traore-Ouedraogo R, Guissou IP, Henschel V, *et al.* Monoolein–water liquid crystalline gels of gentamicin as bioresorbable implants for the local treatment of chronic osteomyelitis: *in vitro* characterization. *Drug Dev Ind Pharm.* 2008;34:753–60.
- Kundu B, Soundrapandian C, Nandi SK, Mukherjee P, Dandapat N, Roy S, *et al.* Development of new localized drug delivery system based on ceftriaxone–sulbactam composite drug impregnated porous hydroxyapatite: a systematic approach for *in vitro* and *in vivo* animal trial. *Pharm Res.* 2010;27:1659–76.
- Balamurugan A, Balossier G, Kannan S, Michel J, Rebelo AH, Ferreira JM. Development and *in vitro* characterization of sol–gel derived CaO–P<sub>2</sub>O<sub>5</sub>–SiO<sub>2</sub>–ZnO bioglass. *Acta Biomater.* 2007;3:255–62.
- Balamurugan A, Balossier G, Laurent-Maquin D, Pina S, Rebelo AH, Faure J, *et al.* An *in vitro* biological and anti-bacterial study on a sol–gel derived silver-incorporated bioglass system. *Dent Mater.* 2008;24:1343–51.
- Zhu Y, Kaskel S. Comparison of the *in vitro* bioactivity and drug release property of mesoporous bioactive glasses (MBGs) and bioactive glasses (BGs) scaffolds. *Micropor Mesopor Mat.* 2009;118:176–82.
- Czarnobaj K. Preparation and characterization of silica xerogels as carriers for drugs. *Drug Deliv.* 2008;15:485–92.



10. Agathopoulos S, Tulyaganov DU, Ventura JMG, Kannan S, Saranti A, Karakassides MA, *et al.* Structural analysis and devitrification of glasses based on the CaO–MgO–SiO<sub>2</sub> system with B<sub>2</sub>O<sub>3</sub>, Na<sub>2</sub>O, CaF<sub>2</sub> and P<sub>2</sub>O<sub>5</sub> additives. *J Non-Cryst Solids*. 2006;352:322–8.
11. Bang H-G, Kim S-J, Park S-Y. Biocompatibility and the physical properties of bio-glass ceramics in the Na<sub>2</sub>O–CaO–SiO<sub>2</sub>–P<sub>2</sub>O<sub>5</sub> system with CaF<sub>2</sub> and MgF<sub>2</sub> additives. *J Ceram Process Res*. 2008;9:588–90.
12. Radev L, Hristov V, Samuneva B, Ivanova D. Organic/inorganic bioactive materials. Part II: *in vitro* bioactivity of collagen-calcium phosphate silicate/wollastonite hybrids. *Cent Eur J Chem*. 2009;7:711–20.
13. Nandi SK, Kundu B, Mukherjee P, Mandal TK, Datta S, De DK, *et al.* *In vitro* and *in vivo* release of cefuroxime axetil from bioactive glass as an implantable delivery system in experimental osteomyelitis. *Ceram Int*. 2009;35:3207–16.
14. Kontonasaki E, Zorba T, Papadopoulou L, Pavlidou E, Chatzistavrou X, Paraskevopoulos K, *et al.* Hydroxy carbonate apatite formation on particulate bioglass *in vitro* as a function of time. *Cryst Res Technol*. 2002;37:1165–71.
15. Hing KA. Bioceramic bone graft substitutes: influence of porosity and chemistry. *Int J Appl Ceram Technol*. 2005;2:184–99.
16. Chai F, Hornez JC, Blanchemain N, Neut C, Descamps M, Hildebrand HF. Antibacterial activation of hydroxyapatite (HA) with controlled porosity by different antibiotics. *Biomol Eng*. 2007;24:510–4.
17. Seeley Z, Bandyopadhyay A, Bose S. Tricalcium phosphate based resorbable ceramics: influence of NaF and CaO addition. *Mat Sci Eng C*. 2008;28:11–7.
18. Orefice R, West J, LaTorre G, Hench L, Brennan A. Effect of long-term *in vitro* testing on the properties of bioactive glass–polysulfone composites. *Biomacromolecules*. 2010;11:657–65.
19. Balamurugan A, Balossier G, Michel J, Kannan S, Benhayoune H, Rebelo AH, *et al.* Sol gel derived SiO(2)–CaO–MgO–P(2)O(5) bioglass system—preparation and *in vitro* characterization. *J Biomed Mater Res B Appl Biomater*. 2007;83:546–53.
20. NCCLS. Performance standards for antimicrobial susceptibility testing. Wayne: NCCLS; 2002.
21. Xia W, Chang J. Well-ordered mesoporous bioactive glasses (MBG): a promising bioactive drug delivery system. *J Control Release*. 2006;110:522–30.
22. Noble L, Gray AI, Sadiq L, Uchegbu IF. A non-covalently cross-linked chitosan based hydrogel. *Int J Pharm*. 1999;192:173–82.
23. Rossi S, Marciello M, Sandri G, Bonferoni MC, Ferrari F, Caramella C. Chitosan ascorbate: a chitosan salt with improved penetration enhancement properties. *Pharm Dev Tech*. 2008;13:513–21.
24. Ubaidulla U, Khar RK, Ahmad FJ, Tripathi P. Optimization of chitosan succinate and chitosan phthalate microspheres for oral delivery of insulin using response surface methodology. *Pharm Dev Tech*. 2009;14:96–105.
25. Kong M, Chen XG, Liu CS, Liu CG, Meng XH, Yule J. Antibacterial mechanism of chitosan microspheres in a solid dispersing system against *E. coli*. *Colloids Surf B: Biointerfaces*. 2008;65:197–202.
26. Park Y, Kim MH, Park SC, Cheong H, Jang MK, Nah JW, *et al.* Investigation of the antifungal activity and mechanism of action of LMWS-chitosan. *J Microbiol Biotechnol*. 2008;18:1729–34.
27. Baldrick P. The safety of chitosan as a pharmaceutical excipient. *Regul Toxicol Pharmacol*. 2010;56:290–9.
28. El-Kamel AH, Baddour MM. Gatifloxacin biodegradable implant for treatment of experimental osteomyelitis: *in vitro* and *in vivo* evaluation. *Drug Deliv*. 2007;14:349–56.
29. Melville A, Rodríguez-Lorenzo L, Forsythe J. Effects of calcination temperature on the drug delivery behaviour of ibuprofen from hydroxyapatite powders. *J Mater Sci Mater Med*. 2008;19:1187–95.